Uplift, Thermal Unrest, and Magma Intrusion at Yellowstone Caldera

Charles W. Wicks[1], Wayne Thatcher[1], Daniel Dzurisin[2] & Jerry Svarc[1]

[1]*U. S. Geological Survey, MS 977, Menlo Park, CA 94555, USA*

[2]*U. S. Geological Survey, David A. Johnston Cascades Volcano Observatory, 1300 S.E. Cardinal Court Bldg. 10, Suite 100 Vancouver, WA 98683, USA*

The Yellowstone caldera, in the western United States, formed ~640,000 years ago when an explosive eruption ejected ~1,000 km[3] of material[1]. It is the youngest of a series of large calderas that formed during sequential cataclysmic eruptions that began ~16 Myr ago in eastern Oregon and northern Nevada. The Yellowstone caldera was largely buried by rhyolite lava flows during eruptions that occurred from ~150,000 to ~70,000 years ago[1]. Since the last eruption, Yellowstone has remained restless, with high seismicity, continuing uplift/subsidence episodes with movements of ~70 cm historically[2] to several metres since the Pleistocene epoch[3], and intense hydrothermal activity. Here we present observations of a new mode of surface deformation in Yellowstone, based on radar interferometry observations from the European Space Agency ERS-2 satellite. We infer that the observed pattern of uplift and subsidence results from variations in the movement of molten basalt into and out of the Yellowstone volcanic system.

In a previous satellite interferometric synthetic aperture radar (InSAR) study of Yellowstone[4], interferograms from 1992 to 1997 revealed a change from caldera-wide subsidence that began in 1985 (ref. 5) to uplift that began in 1995 and by 1997 involved the whole caldera floor (Fig. 1) as well as the area of uplift shown in Fig. 2A. Because the area of uplift in Fig. 2a is under the north caldera rim, we refer to it as the NUA (North rim Uplift Anomaly). Surface movements from 1996 to 2002 have proven to be

even more dynamic (Fig. 2), with important implications for the nature of the magmatic plumbing of Yellowstone caldera and large caldera systems in general. Campaign mode GPS measurements from 1995 to 2000 (ref. 6) first revealed that NUA had become an isolated area of uplift, in agreement with InSAR observations (Fig. 2) that are drawn from all available satellite radar data. As NUA continued to rise after 1995, vertical motion of the caldera floor connecting the two resurgent domes (Sour Creek, SC and Mallard Lake, ML, in Fig. 1) changed from uplift to subsidence between late 1997 and early 1998. NUA continued to inflate as the caldera floor subsided until 2002 at which time both movements ceased, or at least paused (Figs. 2B-D).

In order to model a deformation source for the entire inflation episode at NUA, we formed the interferogram in Fig. 3A by summing the interferograms in Fig. 2A-C. The total amount of volume added by the modelled inflating sill beneath NUA (see Supplementary Information) shown in Fig. 3 is 0.06 to 0.1 km^3. The best-fit model synthetic interferogram is shown in Fig. 3B and the residual is shown in Fig. 3C. In Fig. 3D we show a profile through Y-Y' (Fig. 3A) that passes through the peak uplift at NUA and the peak subsidence at SC. By all appearances, the uplift at NUA and the subsidence of the caldera floor are linked. Therefore, any model that explains the uplift should also explain the subsidence.

Past episodes of uplift and subsidence in the caldera have been attributed to various combinations of the following two processes taking place beneath the caldera. (1) Pressurization and de-pressurization of an alternately self-sealed and leaking hydrothermal fluid reservoir that traps volatiles exsolved from a crystallizing rhyolitic magma[7]. (2) Movement, formation and crystallization of rhyolitic and or basaltic magma.

Ingebritsen et al.[8] noted that Chloride flux measurements at Yellowstone -- which provide a measure of the hydrothermal heat loss -- do not show any obvious temporal changes that might relate to changes in deformation style. This led them to suggest that deep magmatic processes were more likely causes of uplift/subsidence cycles at Yellowstone. Because chloride is one of the volatile species that is exsolved from rhyolitic magma during crystallization, any rupture of a sealed hydrothermal reservoir might be expected to eventually produce a corresponding increase in chloride flux at the surface. The lack of Chloride flux anomalies that are correlated to deformation episodes does not rule out a hydrothermal deformation source, but it is more easily compatible with a magmatic source for deformation.

We propose that the observed patterns of uplift and subsidence result from variations in what may be nearly continuous movement of molten basalt in to and out of the Yellowstone volcanic system. Increases in the rate of basaltic magma flux into the caldera from beneath SC (Fig. 1) favour inflation of the caldera, whereas decreases favour subsidence. Increases in the rate of basaltic magma flux out of the caldera near NGB (Fig. 1) favour subsidence of the caldera, whereas decreases favour inflation. The main driving forces moving the basaltic magma into the system are the integrated buoyancy of the magma and the vertical gradient in normal stress. The combination of extensional stress (Yellowstone is at the northeastern corner of Basin-and-Range extension) and high heat flow present in Yellowstone is expected to favour emplacement of magma at rheological boundaries[9,10]. If the flux of magma is too great, however, it would tend to continue its near vertical ascent[11].

We interpret the beginning of caldera uplift in 1995 as the introduction of a pulse of basaltic magma below SC from a source in the upper mantle. In the subsequent year the uplift spread across the entire caldera[4], including the area of NUA, as the magma spread horizontally at a rheological boundary. Previous studies have inferred the

presence of a partially molten rhyolitic body[1,12-14] that would form a rheological boundary with an accompanying sharp upward decrease in density. As the basalt spreads beneath the caldera, it loses heat to the overlying rock. This heat keeps the geothermal system, and thus the surface hydrothermal features, active.

The basaltic magma escapes the caldera system at the three-way intersection of the northern caldera boundary, the west-northwest striking seismic belt east of the Hebgen Lake fault zone, and the north trending Norris-Mammoth corridor (Fig. 1). The seismic belt is a rift-like zone of north-south extension[15,16] that is a site of minor post-caldera volcanism and extends west to the site of the 1959 Ms (surface wave magnitude) 7.5 Hebgen Lake earthquake. The Norris-Mammoth corridor is a zone of recurrent normal faulting, post-caldera volcanism, and active thermal features that extends north to beyond Mammoth Hot Springs[1].

Magma accumulated beneath the north caldera boundary, leading to continued uplift at NUA even as the larger part of the caldera floor subsided, because, in our interpretation, the outlet was unable to fully accommodate the increased flux of basaltic magma. The flux of magma out of the Yellowstone system is controlled by extra-caldera tectonic activity acting on fractured rock bordering the northern caldera boundary. Tectonic strain can either enhance or restrict the flow of magma out of the caldera. The two largest earthquake swarms recorded in Yellowstone each accompanied, or slightly preceded, the change from caldera-wide uplift to subsidence in 1985, and the change from caldera-wide subsidence to a brief episode of caldera-wide uplift in 1995 (refs. 4, 17). A similar scenario has been suggested at Loihi volcano in Hawaii[18] where a 1996 earthquake swarm was associated with magma chamber drainage, and a 2001 earthquake swarm was associated with magma chamber filling. The shallower southeastern end of the dipping sill that models the inflation at NUA is at the same depth as the two deflating sills it intersects beneath the caldera floor. The

dipping sill deepens to the north-northwest by ~7 km at the proposed outlet effectively

forming a trap for the now negatively buoyant magma. Inclusion of GPS data[6] in a joint

inversion of GPS and InSAR data (Supplementary Information) yields a similarly

oriented prolate spheroid as an allowable model. Adoption of the spheroid does not

change the proposed path of magma migration, but rather the mode of migration to one

more pipe-like in nature. As the magma leaves the caldera, it could become negatively

buoyant via three separate processes: 1) cooling, 2) crystallization, and 3) degassing of

CO_2. The denser magma might then be emplaced in a large 10-km-thick sill inferred in

ref. 19.

Inflation beneath NUA has led to extensive dilatation of the upper crust (Fig. 4).

In faulted and fractured areas, such as geyser basins, this could lead to a dramatic

increase in permeability. The 2000-01 interferogram (Fig. 2B) shows several small (2-5

km) areas of inflation with ~30-50 mm of peak amplitude north of NUA in the highly

faulted, thermally active Mammoth-Norris corridor, which may be atmospheric delay

artefacts. However, drawing on the results of a study by Hanssen et al.[20] and ground

based radar (see Supplementary Information), it is more likely that these are areas of

local inflation. These areas are also absent in the 1996-2000 interferogram (Fig. 2A),

and they have broadened and extended northward in 2001-02 (Fig. 2C) to occupy the

entire Mammoth-Norris corridor. We suggest the dilatation opened new or healed

fractures or increased permeability in existing fractures, resulting in better

communication between the shallow thermal systems and the deeper geothermal

reservoir thus forming the small-scale areas of inflation.

Thermal disturbances in Norris Geyser basin (Figs. 1, 4) are near-annual events

that have been related to yearly water table lows[21]. The thermal disturbances have

recently become more pronounced (see Supplementary Information), perhaps in

response to dilatation from NUA. Ingebritsen and Rojstaczer[22] have demonstrated that

the permeability of a geyser's fracture zone conduit may be an important factor in the eruption frequency of a geyser. Dilatation from NUA is thus a possible mechanism for increasing permeability in the geyser conduits, thereby increasing geyser eruption frequency. Husen et al[23] noted an increase in geyser eruption frequency within hours after surface waves from the 2002 Denali earthquake produced ~0.5 microstrain of dynamic strain at Yellowstone. We calculate strains an order of magnitude greater (>6 microstrain) applied over a time interval 4 orders of magnitude longer (~3-4 years). Inertial forces are insignificant for the dilatation we calculate, but there must be competition between 1) opening of cracks by hydro-fracturing and 2) healing of cracks through mineral precipitation and annealing that, beginning in 2000, led to the manifestation of shallow responses to the dilatation.

The episode of accentuated thermal unrest in the near-annual disturbances from 2000-03 is not unique in the recorded history of Yellowstone National Park[21]. It is unique, however, that for this episode we have been able to use InSAR to track changes in the deformation field in the park during the unrest that suggest a cause and effect relationship. Indeed, past episodes of accentuated thermal unrest during near-annual disturbances in Norris Geyser basin may also have been caused by dilatation related to uplift from magma accumulation at depth, but in the absence of geodetic monitoring, earlier deformation episodes would have gone undetected.

1. Christiansen, R. L. The Quaternary and Pliocene Yellowstone Plateau Volcanic field of Wyoming, Idaho, and Montana. *US Geol. Surv. Prof. Pap. 729-G*, 1-145 (2001).

2. Pelton, J. R. & Smith, R. B. Recent crustal uplift in Yellowstone National Park. *Science*, **206**, 1179-1182 (1979).

3. Pierce, K. L., Cannon, K. P., Meyer, G. A., Trebesch, M. J. & Watts, R. D. Post-Glacial Inflation-Deflation Cycles, Tilting, and Faulting in the Yellowstone Caldera Based on Yellowstone Lake Shorelines. *US Geol. Surv. Open-File Rept. 02-0142*, 1-62, (2002).

4. Wicks, C., Thatcher, W. & Dzurisin, D. Migration of fluids beneath Yellowstone Caldera inferred from satellite radar interferometry. *Science* **282**, 458-462 (1998).

5. Dzurisin, D., Savage, J.C. & Fournier, R. O. Recent crustal subsidence at Yellowstone caldera, Wyoming. *Bull. Volcanol.* **52**, 247-270 (1990).

6. Meertens, C. M., Smith, R. B. & Puskas, C. M. Crustal deformation of the Yellowstone caldera from campaign and continuous GPS surveys, 1987-2000. *Eos* **81**(48) V22F-19 (2000).

7. Fournier, R. O. Hydrothermal processes related to movement of fluid from plastic into brittle rock in the Magmatic-epithermal environment. *Econ. Geol.* **94**, 1193-1211 (1999).

8. Ingebritsen, S. E., Galloway, D. L., Colvard, E. M., et al. Time-variation of hydrothermal discharge at selected sites in the western United States: implications for monitoring. *J. Volcanol. and Geotherm. Res.* **111**, 1-23 (2001).

9. Rubin, A. M. Propagation of magma-filled cracks. *Annu. Rev. Earth Planet. Sci.* **23**, 287-336, (1995)

10. Watanabe, T., Koyaguchi, T. & Seno, T. Tectonic stress controls on ascent and emplacement of magmas. *J. Volcanol. Geotherm Res.* **91**, 65-78, (1999).

11. Dahm, T. Numerical simulations of the propagation path and the arrest of fluid-filled fractures in the Earth. *Geophys. J. Int.* **141**, 623-638 (2000).

12. Eaton, G. P., Christiansen, R. L., Iyer, H. M., Pitt, A. M., et al. Magma beneath Yellowstone National Park. *Science*, **188**, 787-796 (1975).

13. Miller, D. S. & Smith, R. B. P and S velocity structure of the Yellowstone volcanic field from local earthquake and controlled source tomography. *J. Geophys. Res.* **104**, 15105-15121, (1999).

14. Husen, S., Smith, R. B. & Waite, G. P. Evidence for gas and magmatic sources beneath the Yellowstone volcanic field from seismic tomographic imaging. *J. Volcanol. Geotherm. Res.* **131**, 397-410 (2004).

15. Savage, J. C., Lisowski, M., Prescott, W. H. & Pitt, A. M. Deformation from 1973 to 1987 in the epicentral area of the 1959 Hebgen Lake, Montana, earthquake ($M_s =$ 7.5). *J. Geophys. Res.* **98**, 2145-2153, (1993).

16. Waite, G. P. & Smith, R. B. Seismotectonics and stress field of the Yellowstone volcanic plateau from earthquake first-motions and other indicators. *J. Geophys. Res.* **109**, doi:10.1029/2003JB002675 (2004).

17. Waite, G. P. & Smith, R. B. Seismic evidence for fluid migration accompanying subsidence of the Yellowstone Caldera. *J. Geophys. Res.* **107**, doi:10.1029/2001JB000586 (2002).

18. Wolfe, C. J., Okubo, P. G., Ekström, G., Nettles, M. & Shearer, P. M. Characteristics of deep (≥13 km) Hawaiian earthquakes and Hawaiian earthquakes west of 155.55°W. *Geochem. Geophys. Geosyst.* **5**, doi:10.1029/2003GC000618 (2004).

19. Humphreys, E. D., Dueker, K. G., Schutt, D. L. & Smith, R. B. Beneath Yellowstone: Evaluating plume and nonplume models using teleseismic images of the upper mantle. *GSA Today* **10**, 1-7 (2000).

20. Hanssen, R. F.; Weckwerth, T. M., Zebker, H. A. & Klees, R. High-Resolution Water Vapor Mapping from Interferometric Radar Measurements. *Science*. **283**, 1297-1299, (1999)

21. White, D. E., Hutchinson, R. A. & Keith, T.E.C. The geology and remarkable thermal activity of Norris Geyser Basin, Yellowstone National Park, Wyoming. *U. S. Geol. Surv. Prof. Paper* **1456,** 1-84 (1988).

22. Ingebritsen, S. E. & Rojastaczer, S. A. Controls on Geyser Periodicity. *Science* **262**, 889-892 (1993).

23. Husen, S., Taylor, R., Smith, R. B. & Heasler, H. Changes in geyser eruption behavior and remotely triggered seismicity in Yellowstone National Park produced by the 2002 M 7.9 Denali fault earthquake, Alaska. *Geology* **32**, doi:10.1130/G20381.1 (2004).

24. Massonnet, D. & Feigl, K. L. Radar interferometry and its application to changes in the Earth's surface. *Rev. Geophys.* **36**, 441-500, (1998).

25. Toda, S., Stein, R. S., Reasenberg, P. A. & Dieterich, J. H. Stress transferred by the *Mw*=6.9 Kobe, Japan, shock: Effect on aftershocks and future earthquake probabilities, *J. Geophys. Res.*, **103**, 24,543-24,565 (1998).

Figure 1 | A map of structural, thermal and volcanic features in and around Yellowstone caldera. (Map taken from Christiansen[1].) The red symbols mark volcanic centres that erupted after the caldera forming event 640 kyr ago. The areas of known past or present thermal activity are coloured yellow. The ring-

fracture zone of the caldera is shown green, and the slumped zone between the ring-fracture zone and the best estimate of the caldera rim is shown salmon. The park boundary is the dashed black line. Faults active in the Quaternary are marked with black lines. The labelled features are Norris Geyser Basin (NGB), Mammoth Hot Springs (M), Sour Creek Dome (SC), Mallard Lake dome (ML), Hebgen Lake (HL), and Yellowstone Lake (YL). The semitransparent white arrows show interpreted magma migration paths. The red square in the inset map (bottom right) shows the location of the study area.

Figure 2 | **Four interferograms showing the deformation during the episode of uplift at NUA.** A colour change from violet to blue to green to yellow to red marks an increase in the range (distance from the satellite to points on the ground) of 28.3 mm. The white circles represent epicentres of earthquakes recorded during the time interval spanned by each interferogram. The interferograms have been generated using European Space Agency ERS-2 data (see Supplementary Information) and the two-pass method of interferometry[24]. The extensive double dash length broken line in each panel shows the boundary of Yellowstone National Park. The short dash length broken line in each panel (within the park boundary) shows the approximate location of the 640,000-year-old caldera rim. **A**, Summer 1996 to summer 2000 interferogram. Although the caldera floor appears to have subsided only slightly, this period includes about 30 mm of caldera-wide uplift from 1996 to 1997 (ref. 4). Therefore, more than 30 mm of subsidence of the caldera floor occurred between the two resurgent domes from 1997 to 2000. **B**, Summer 2000 to summer 2001 interferogram. **C**, Summer 2001 to summer 2002 interferogram. **D**, Summer 2002 to summer 2003 interferogram.

Figure 3 | **Observed and modelled uplift at NUA and subsidence of caldera floor.** The black outlines are the surface projections of a north-northwest trending expanding sill, and two northeast trending contracting sills. Dashed line is the outline of Yellowstone National Park. **A**, A stacked interferogram formed by summing unwrapped versions of the interferograms in Fig. 2A-C. **B**, Synthetic interferogram from best-fit model. **C**, Residual interferogram formed by subtracting the synthetic interferogram (**B**) from the observed interferogram (**A**). **D**, Deformation profiles from Y to Y'. The colours denote: blue, 1996-2000 deformation, cyan, 1996-2001 deformation, green, 1996-2002 deformation, black, 2002-03 deformation, and red, deformation from best-fit model (**B**). Elevation along the profile is shown by the black dotted line.

Figure 4 | **Dilatation calculated from the inflating sill in Fig. 3.** (Calculations were performed using Coulomb 2.5; ref. 25.) **A**, Dilatation at the surface resulting from the NUA uplift episode. The arrow labelled 'NGB' marks the location of Norris Geyser basin and the arrow labelled 'Nymph Lake' marks the location of the newly formed line of fumaroles near Nymph Lake. The black-dash line is the approximate caldera rim. The black lines are mapped faults active in the Quaternary[1]. The black rectangle is the surface projection of the best-fit expanding sill. **B**, Cross-section through X-X' in (**A**) resulting from the uplift episode. The peak dilatation is just under 7 microstrain at the surface. The cyan circles show earthquakes greater than M=0.0 that occurred before the uplift episode (1 Jan. 1992 through to 31 Dec. 1997) and the red circles show earthquakes greater than M=0.0 that occurred during the uplift episode (1 Jan. 1998 through to 13 Aug. 2003). Earthquakes 10 km each side of the X-X' line are projected onto the cross-section. Size of circles is scaled to earthquake magnitude. Note that for better visualization, this scaling is different for the red

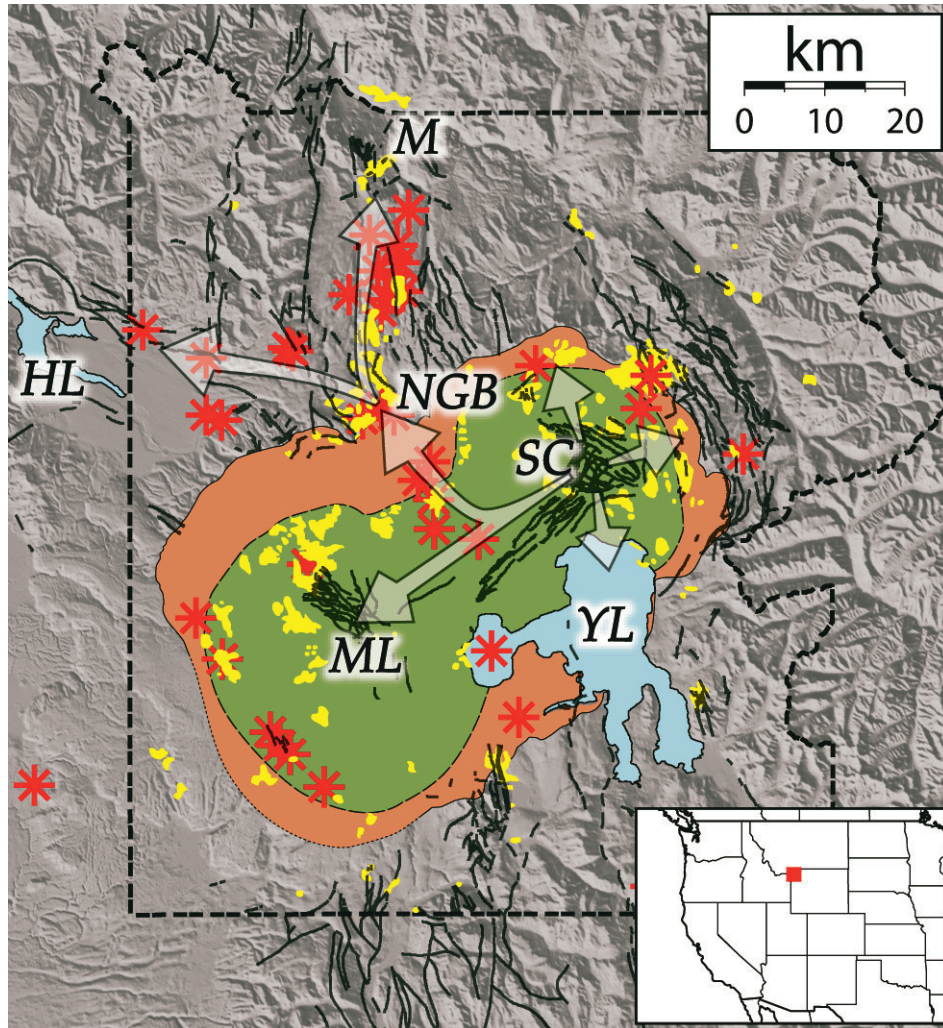and cyan circles; for two earthquakes with the same magnitude (one cyan, one red), the red circle plots at twice the diameter of the cyan circle.
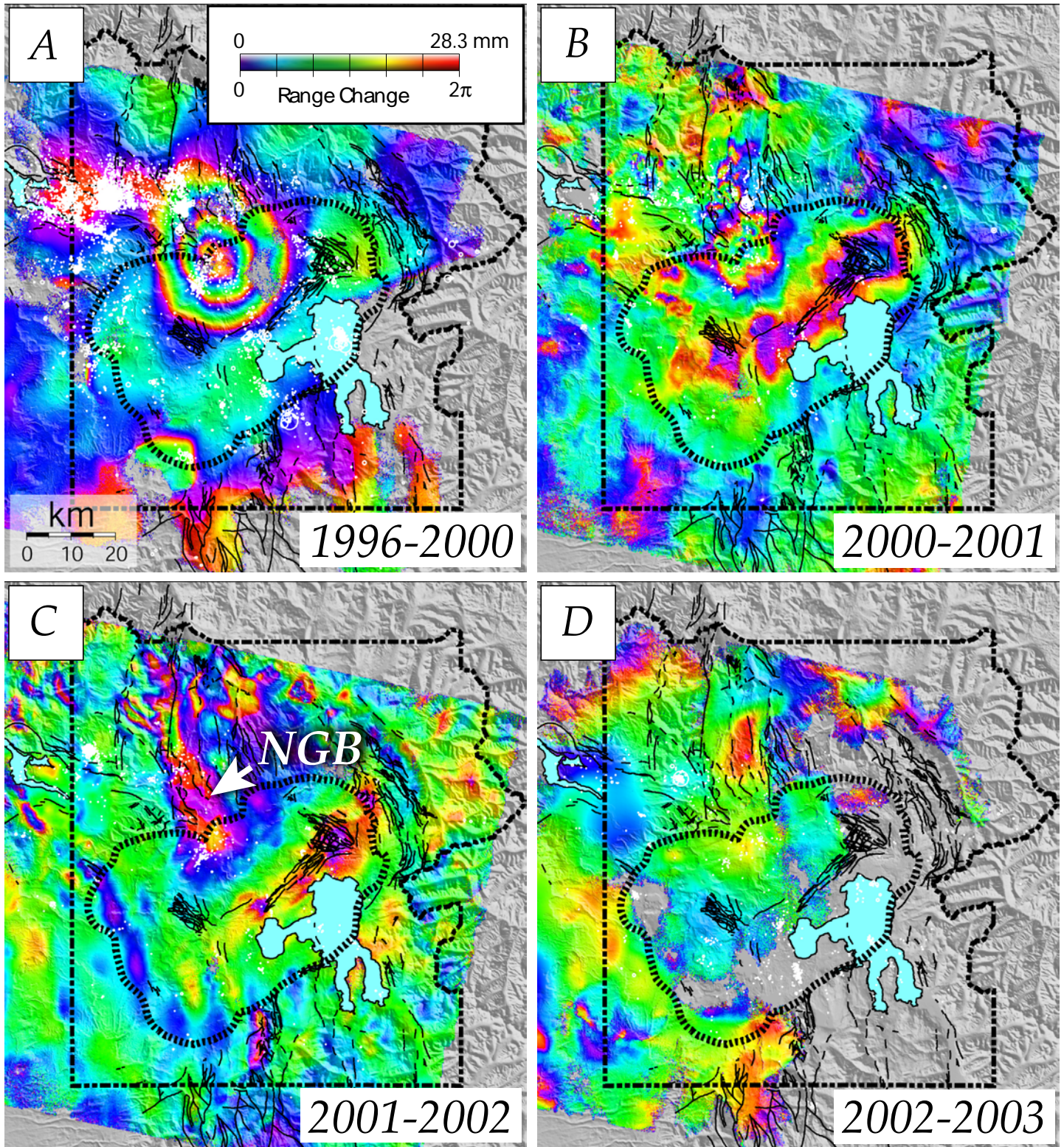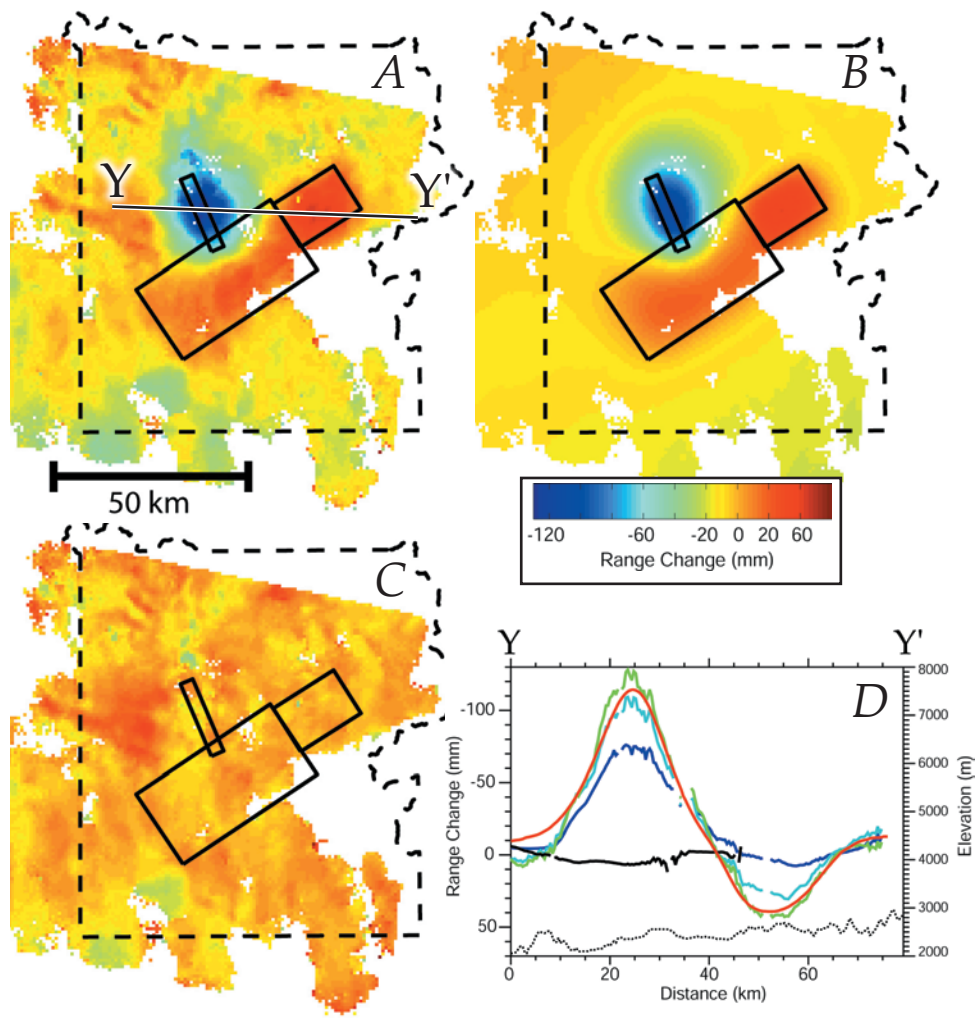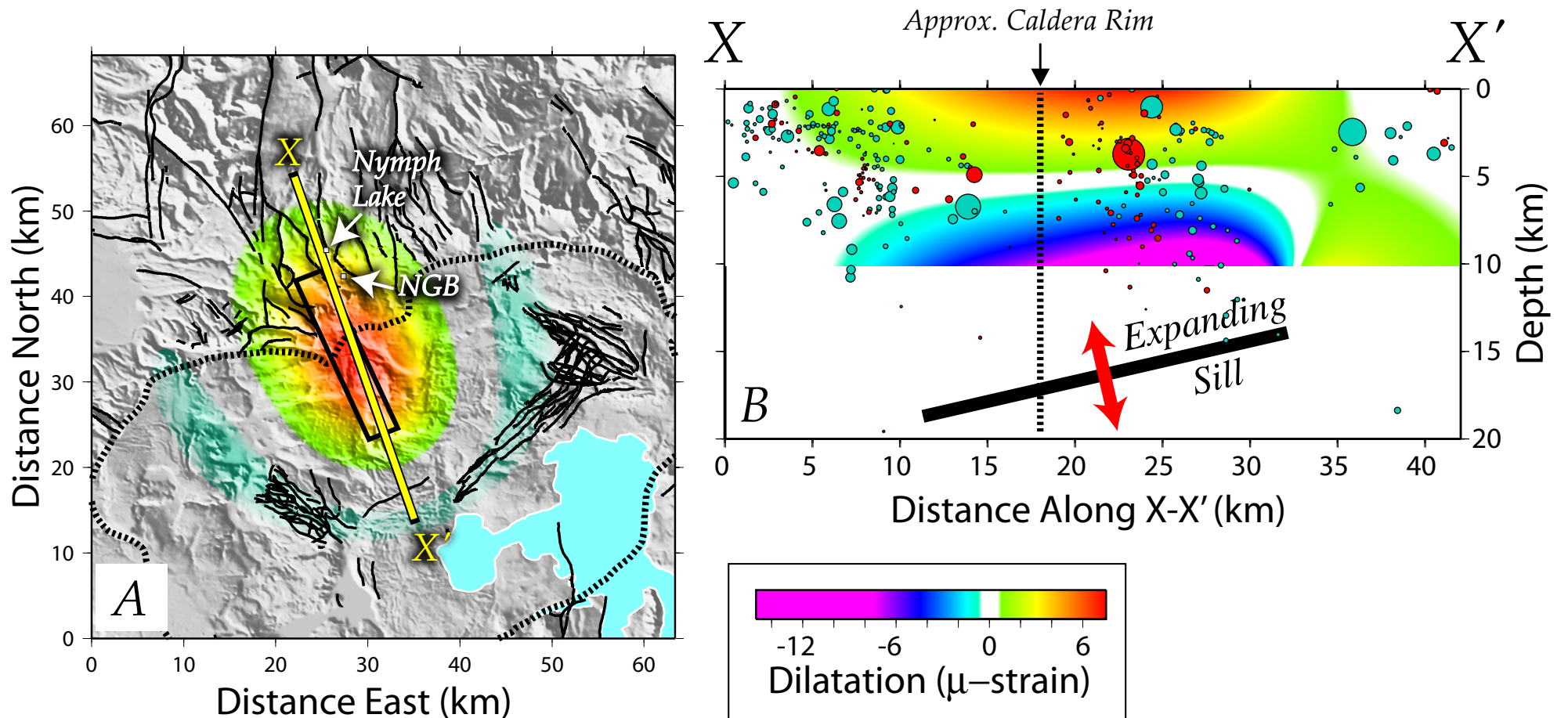
Figure 1

Fig. 2

Fig. 3

Fig. 4